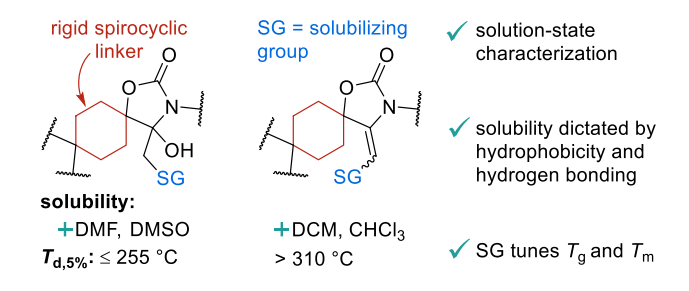
Improved Characterization of Polyoxazolidinones by Incorporating Solubilizing Side Chains

Allison R. Wong, Melissa Barrera, Arpan Pal, Jessica R. Lamb*

Department of Chemistry

University of Minnesota—Twin Cities

207 Pleasant Street SE, Minneapolis, MN 55455 (USA)



For Table of Contents use only

SUBJECTS: Chemical structure, Degradation, Polymers, Solubility, Solvents

Abstract. Carbon dioxide-based polyoxazolidinones (POxa) are an emerging subclass of non-isocyanate polyurethanes for high temperature applications. Current POxa with rigid linkers suffer from limited solubility that hinders synthesis and characterization. Herein, we report the addition of alkyl and alkoxy solubilizing groups to rigid spirocyclic POxa and their poly(hydroxyoxazolidinone) (PHO) precursors. The modified polymers were soluble in up to six organic solvents, enabling characterization of key properties (e.g., molar mass and polymer

structure) using solution-state methods. Dehydration of PHO to POxa changed solubility from highly polar to less polar solvents and improved thermal stability by 76–102 °C. The POxa had relatively high glass transition (85–119 °C) and melting (190–238 °C) temperatures tuned by solubilizing group structure. The improved understanding of factors affecting solubility, structure–property relationships, and degradation pathways gained in this study broadens the scope of soluble POxa and enables more rational design of this promising class of materials.

Introduction. Polyurethanes (PUs) are commonly used in an expansive range of commercial products, 1,2 including foams, 3 coatings, 4,5 and elastomers. Polyoxazolidinones (POxa) are an emerging subclass of PUs with five-membered cyclic urethanes (oxazolidinones) embedded in the polymer backbone. These oxazolidinone linkages impart POxa with high thermal stability $^{7-11}$ and glass transition temperatures (T_g)⁸⁻¹⁴ which make them promising for high-temperature engineering thermoplastic applications. 9,12 Unfortunately, the traditional synthesis of POxa from the step-growth polymerization of diisocyanates and diepoxides 15,16 has many drawbacks, including high reaction temperatures (>150 °C), 9,12 lack of regioselectivity, 12,13 and undesired side reactions (e.g., isocyanate trimerization to form isocyanurate cross-links). 9,12,17 Additionally, the environmental 18 and health 19 concerns of isocyanates have resulted in increased regulation, 20 necessitating the development of alternative, non-isocyanate routes to these materials.

To address these concerns, non-isocyanate POxa have been reported via (1) polycondensation of diurethanes and diepoxides, ^{15,21} (2) cyclization of poly(propargylamine)s with CO₂, ^{10,22–24} and (3) polyaddition of CO₂-based bis(α-alkylidene cyclic carbonate)s (bisαCCs)²⁵ and diamines to form poly(hydroxyoxazolidinone)s (PHO) followed by dehydration. ^{11,26} Routes 2 and 3 are particularly attractive because CO₂ is a nontoxic, renewable, abundant, and inexpensive C1 feedstock. ^{27,28}

Investigations into CO₂-based PHO and POxa have been hindered by inconsistent solubility in common organic solvents. Their solubility strongly depends on the structure of the linkers (Figure 1A): polymers with two flexible linkers are typically soluble 11,26 whereas the inclusion of more rigid linkers (e.g., aromatic or aliphatic rings) often results in insoluble polymers. This insolubility limits the development of rigid POxa—which are expected to have higher $T_g^{11,12,14}$ —because the polymers precipitate during the polymerization and key properties (e.g., molar mass) cannot be characterized using common solution-state methods. Therefore, a more general strategy is required to access soluble PHO and POxa with diverse linkers and expand the utility of these materials.

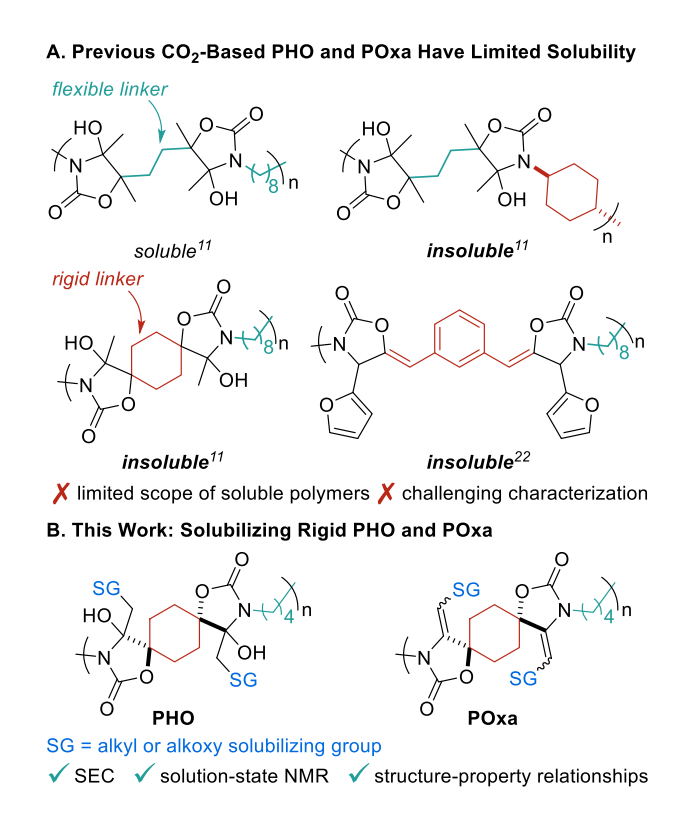


Figure 1. (A) Limited solubility of previous CO₂-based PHO¹¹ and POxa²² with rigid linkers. (B) Addition of SGs to rigid spirocyclic PHO and POxa.

Herein, we address this limitation by incorporating alkyl or alkoxy solubilizing groups (SGs) into PHO and POxa with a rigid spirocyclic linker (Figure 1B). The modified polymers not only exhibited improved and tunable solubility in organic solvents but also revealed differences in the primary influence underlying solubility between the two scaffolds. Thermal analyses provided insight into (1) the contrast between PHO and POxa thermal degradation and (2) structure—property relationships of POxa with variable SG identities. This deeper fundamental understanding will enable more rational design of this promising class of materials.

Results and Discussion

Selection of the Model System and Monomer Synthesis. The addition of SGs to PHO and POxa was inspired by the field of conjugated polymers in which solubilizing side chains are well-known to successfully prevent aggregation and improve solubility.^{29–34} To see the most pronounced effects from the incorporation of SGs, we sought a highly insoluble model system with a rigid linker. Therefore, the previously reported spirocyclic bisαCC monomer¹¹ was an obvious choice because it resulted in insoluble polymers even when paired with flexible 1,8-diaminooctane. Additionally, the bisαCC-diamine route facilitates the incorporation of SGs and can utilize potentially renewable feedstocks, such as CO₂,^{27,28} 1,4-diaminobutane,^{35,36} and 1,4-cyclohexanedione.^{37,38}

The SGs were introduced as substituents on terminal alkynes, starting with a series of linear alkyl groups (Scheme 1, SG = C3, C5, and C10) to investigate the effect of chain length on solubility. We also included 2-ethylhexyl ether (EHE) as a SG because the greater steric bulk of its branched structure is known to improve solubility of conjugated polymers compared to linear alkyl chains.^{32,39} We acknowledge the EHE ether linkage may have additional implications on

polymer properties, but it was required for synthetic accessibility (see the Supporting Information for more details).

Scheme 1. Synthesis of BisaCC Monomers

We synthesized the bis α CC monomers in two steps, starting with the double addition of terminal alkynes to 1,4-cyclohexanedione to gain access to diastereomerically pure *trans*-bis(propargyl alcohol)s (Scheme 1; see the Supporting Information for full experimental details).⁴⁰ Subsequent silver-catalyzed cyclization with CO₂ resulted in bis α CC monomers.⁴¹ Single crystal X-ray crystallography analysis of ^{C5}bis α CC confirmed the *trans* configuration of the cyclohexyl linker and *E* configuration of the exocyclic alkenes (Figure S33).

Polymer Synthesis and Structural Characterization. We polymerized this library of bisαCC monomers with 1,4-diaminobutane at 80 °C using catalytic 1,8-diazabicyclo[5.4.0]undec-7-ene (DBU) to form PHO (Table 1; see Table S1 for polymerization optimization). While this type of polymerization has been reported at room temperature without a catalyst, 11 we used elevated temperatures and DBU because these conditions resulted in higher molar mass polymers that should highlight the effect of SGs. Unlike the previously reported spirocyclic PHO, 11 the SG-containing polymers remained soluble in DMF throughout the polymerization, enabling molar mass determination using size exclusion chromatography with multi-angle light scattering (SEC-

MALS). The PHO (SG = C3, C5, and EHE) had number average molar masses (M_n) of 9.2–20.9 kDa and dispersities (D) of 1.42–1.78 (Table 1). The molar mass of C^{10} PHO was determined using poly(methyl methacrylate) (PMMA) standards instead of MALS due to insolubility of the purified polymer (*vide infra*) that prevented measurement of dn/dc. The molar mass of this polymer therefore could not be directly compared to the other PHO. The use of a MALS detector for absolute molar mass determination is particularly important for these materials because the presence of backbone rings is expected to drastically change the hydrodynamic volume such that refractive index (RI) detectors versus standards will not be accurate. Indeed, we observed a 3–8 kDa overestimation of M_n when measured by PMMA standards compared to MALS (Table S2).

Table 1. Synthesis of PHO

$$\begin{array}{c} \text{SG} \\ \text{O} \\ \text$$

polymer	M_n^a (kDa)	$M_{\rm w}^{\rm a}$ (kDa)	Đª	DP ^b
^{C3} PHO	9.2	13.0	1.42	22
^{C5} PHO	9.8	14.7	1.50	20
^{C10} PHO	10.4°	16.7°	1.61 ^c	17°
ЕНЕРНО	20.9	37.3	1.78	33

^aMolar mass and \mathcal{D} of crude PHO were determined using SEC–MALS in DMF with LiBr at 40 °C. ^bDegree of polymerization (DP) derived from M_n . ^cMolar mass, \mathcal{D} , and DP were determined using SEC versus PMMA standards.

After confirming SGs solubilized PHO enough to measure molar mass by SEC, we turned our attention to other key properties that can be characterized using solution-state methods. While solid-state ¹³C NMR spectroscopy has been used to investigate the structure of insoluble POxa, ^{11,22} this technique has multiple drawbacks, including high cost, long experiment time, and low resolution with standard instrumentation. ⁴² Gratifyingly, the modified PHO were soluble in DMSO, enabling solution-state ¹H, ¹³C, COSY, HSQC, and HMBC NMR spectroscopy (Figures S5–S7). These analyses confirmed the expected polymer structure without defects.

The observed solubility in DMF and DMSO is particularly impressive considering both the relatively short four-carbon diamine linker and the stereoregularity of the spirocyclic linker. Both of these factors are expected to lead to increased aggregation^{43–45} compared to the insoluble literature system that used both a more flexible eight-carbon diamine and a presumed mixture of bisαCC stereoisomers.¹¹ This contrast highlights the dramatic solubilizing power of SGs for these types of polymers.

Having established that SGs improve solution-state characterization of PHO, we then investigated the effect of these groups on POxa. PHO with alkyl SGs were readily dehydrated to form POxa at room temperature using catalytic acid (Table 2), improving upon reported conditions that required high temperature, excess acid, or both. 11,46 Because of changes in solubility following dehydration (*vide infra*), POxa molar masses (M_n = 2.8–8.3 kDa) were determined in CHCl₃ using polystyrene (PS) standards. Therefore, these values could not be directly compared to the PHO precursors. NMR spectroscopy in CDCl₃ (Figure S11 and Section 4H in the Supporting Information) showed the exocyclic alkene favored the *E* configuration (E:Z=6.0:1-6.6:1), likely due to allylic 1,3-strain⁴⁷ between the SG and the diamine linker.

Table 2. Dehydration of PHO with Alkyl SGs to POxa

polymer	M _n ^a (kDa)	$M_{\rm w}^{\ a} ({\rm kDa})$	Đª	$E:Z^{b}$
^{C3} POxa	3.6	7.0	1.93	6.6:1
^{C5} POxa	2.8	5.8	2.06	6.0:1
^{C10} POxa	8.3	14.0	1.69	6.2:1

^aMolar mass and *D* of purified POxa were determined using SEC in CHCl₃ at 40 °C against PS standards. ^bDetermined from 1D ¹H and 2D NOESY NMR spectroscopy.

Unfortunately, acidic conditions resulted in the elimination of 2-ethyl-1-hexanol from ^{EHE}PHO instead of water to form ^{CH2}PHO (Scheme 2; see Figures S12 and S13 for characterization). As expected, ^{CH2}PHO, which lacks an SG, could not be characterized using solution-state methods due to insolubility in NMR and SEC solvents (*vide infra*). While undesired in this study, this result demonstrates the possibility for SG-clipping strategies for post-polymerization modification of solubility in the future.

Scheme 2. Elimination of 2-Ethyl-1-hexanol from EHEPHO to Form CH2PHO

EHOH = 2-ethyl-1-hexanol

Effect of Polymer Structure on Solubility. Having accomplished the goal of improving solution-state characterization of rigid PHO and POxa, we wanted to test the limits of this approach and better understand the factors underlying solubility. Therefore, we tested their room temperature solubility in six common organic solvents (Table 3; see the Supporting Information for experimental details) using three semiquantitative categories defined by You and co-workers:³⁴ soluble (\geq 10 mg/mL), partially soluble (1–10 mg/mL), and insoluble (<1 mg/mL). The solvents had a range of polarities (dipole moment (μ) = 0.6–4.0 D)^{48,49} as well as Kamlet–Taft parameters of hydrogen bond donor (α = 0–1.96) and acceptor (β = 0–0.76) ability.⁵⁰ Solvents with higher Kamlet–Taft parameters can more easily form hydrogen bonds to polymer chains, disrupting polymer–polymer hydrogen bonding and facilitating dissolution.^{51–53}

Table 3. Semiquantitative Solubility of PHO and POxa at Room Temperature^a

		CHCl ₃	DCM	DCM / DMSO ^b	THF	HFIP	DMF	DMSO
	μ (D)	1.0^{48}	1.648		1.8^{48}	$0.6-3.2^{c,49}$	3.8^{48}	4.0^{48}
	α/β	$0.44/0^{50}$	$0.30/0^{50}$		$0/0.55^{50}$	$1.96/0^{50}$	$0/0.69^{50}$	$0/0.76^{50}$
PHO	C3					++	++	++
	C5			++		++	++	++
	C10			++				
	EHE	++	++	++	++	++	++	++
	CH2							
POxa	С3	++	++	n.d. ^d	++	++		
	C5	++	++	$n.d.^d$	+-	++		
	C10	++	++	n.d. ^d				

^a[green ++] = soluble (≥10 mg/mL), [orange +-] = partially soluble (1–10 mg/mL), [red --] = insoluble (<1 mg/mL). ^bDCM:DMSO = 5:1, v/v. ^cHFIP μ is conformation dependent. ^dn.d. = not determined.

The incorporation of short alkyl SGs fully solubilized ^{C3}PHO and ^{C5}PHO in HFIP, DMF, and DMSO (Table 3), which are strongly polar and can easily disrupt hydrogen bonding. Conversely,

these polymers remained insoluble in solvents with lower polarity and Kamlet–Taft parameters (i.e., CHCl₃, DCM, and THF). ^{C10}PHO was insoluble in all solvents tested, which was surprising because longer SGs typically improve the solubility of conjugated polymers. ^{31,54} We hypothesize this anomaly arises from the combination of (1) hydrophobicity imparted by C10 SGs and (2) hydrogen bonding ability of the pendent hydroxyl groups; the hydrophobicity prevented solubility in more polar solvents whereas the less polar solvents were unable to disrupt polymer–polymer hydrogen bonding. Indeed, the addition of DMSO as a cosolvent to DCM (DCM:DMSO = 5:1, v/v) resulted in the full dissolution of ^{C10}PHO. ^{C5}PHO was also soluble in the cosolvent mixture but ^{C3}PHO was not, highlighting the interplay between polarity and hydrogen bond disruption.

In contrast to the above polymers, ^{EHE}PHO dissolved in all solvents tested (Table 3). We hypothesize the branched EHE structure may result in greater spacing between polymer chains, ^{32,33,55} which could facilitate solvent intercalation and physically separate the pendent hydroxyl groups. This separation would lessen the requirement for hydrogen bond disruption, extending solubility to less polar solvents (i.e., CHCl₃, DCM, and THF) as expected for this hydrophobic SG. After elimination of the EHE group, the resulting ^{CH2}PHO was insoluble in all cases, emphasizing the importance of SGs in facilitating dissolution of rigid PHO.

Following dehydration to POxa, the solubility of all three polymers with alkyl SGs greatly changed, losing solubility in DMF and DMSO and gaining solubility in CHCl₃ and DCM (Table 3). The loss of the hydroxyl groups both eliminated the need for hydrogen bond disruption and reduced the overall polarity of the polymers. We hypothesize the *trans* configuration of the cyclohexyl linker orients the oxazolidinone rings in opposition to each other, minimizing the overall POxa dipole moment and favoring solubility in less polar solvents. The length of the alkyl SG affected POxa solubility in solvents with intermediate polarity (i.e., THF and HFIP) with

solubility decreasing as the length and hydrophobicity of the SG increased. These lessons about the principal determinants of solubility for PHO and POxa expands beyond our original design for the disruption of aggregation inspired by conjugated polymers.^{31–33,39} Overall, these results underscore the nuanced relationship between polymer structure and solubility.

Effect of Polymer Structure on Thermal Properties. Next, we explored the relationship between structure and thermal properties for the modified PHO and POxa. Thermal gravimetric analysis (TGA) showed C3 PHO had a decomposition temperature at 5% weight loss ($T_{d.5\%}$) of 238 $^{\circ}$ C and exhibited a three-stage degradation (Figure 2, solid blue curve), as evident by the three peaks in the weight loss derivative (Figure 2, dashed blue curve). Decreasing the heating rate from 10 to 2 $^{\circ}$ C/min still resulted in a three-stage degradation with a slightly lower $T_{d.5\%}$ of 221 $^{\circ}$ C (Figure S26). The corresponding C3 POxa had a $T_{d.5\%}$ of 314 $^{\circ}$ C—an improvement of 76 $^{\circ}$ C—with a single-stage degradation (Figure 2, solid red curve). The other SGs resulted in similar trends in which the PHO (SG = C5, C10, EHE, and CH2) had $T_{d.5\%}$ of 179–255 $^{\circ}$ C with multistage degradations (Figures S14–S18) and the POxa (SG = C5 and C10) had $T_{d.5\%}$ of 345–346 $^{\circ}$ C with single-stage degradations (Figures S19–S21). These thermal stabilities were comparable to previously reported PHO¹¹ and POxa, 9,11,14,23 indicating that the addition of SGs is not detrimental to thermal stability.

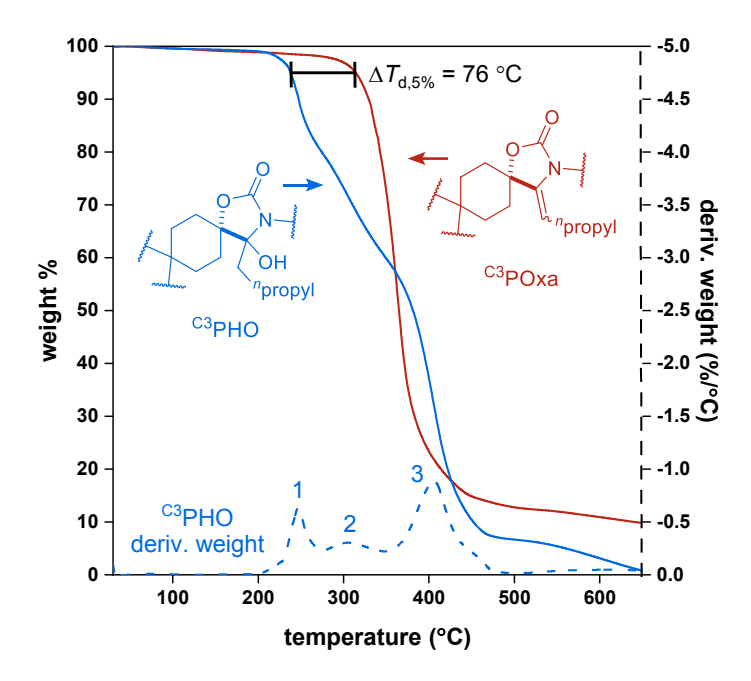


Figure 2. TGA thermograms (10 °C/min) showing the lower thermal stability of ^{C3}PHO (blue) compared to ^{C3}POxa (red). The derivative of ^{C3}PHO weight loss is shown with a dashed blue line to highlight the three-stage degradation.

To better understand the lower thermal stability of PHO compared to POxa, we sought to investigate the degradation pathways of PHO. TGA–mass spectrometry (TGA–MS) analysis of ^{C3}PHO (see Section 2I of the Supporting Information) supported the occurrence of multiple degradation pathways, including partial dehydration to POxa^{11,46} and reversion to oxourethanes (Scheme 3). The oxourethane structure is an intermediate in PHO synthesis (Scheme S1)^{11,26} and contains acyclic urethanes with lower thermal stability than the corresponding cyclic oxazolidinones.^{7,56} The POxa lack pendent hydroxyl groups; therefore, they cannot undergo these pathways, presumably resulting in the higher thermal stability relative to PHO.

Scheme 3. Proposed Thermal Reversion of Hydroxyoxazolidinones to Oxourethanes

The PHO and POxa were also characterized using differential scanning calorimetry (DSC) to determine the effect of SG structure on $T_{\rm g}$ and melting temperature ($T_{\rm m}$). Low thermal stability limited PHO analysis to <100 °C, and no thermal transitions were detected for any polymer (Figure S27). The higher thermal stability of POxa enabled comprehensive DSC analysis. Increasing the SG length by two carbons from C3 to C5 resulted in a 34 °C decrease in $T_{\rm g}$ from 119 to 85 °C (Figure 3). These values are comparable to previously reported POxa with nonaromatic linkers, indicating that relatively high $T_{\rm g}$ can be maintained while enabling characterization in organic solvents. We did not detect a $T_{\rm g}$ for C10POxa from -100 to 250 °C (Figure 3 and S28), which could be due to a $T_{\rm g}$ outside this temperature range, a transition that is too broad for detection, or small amorphous domains caused by high crystallinity (*vide infra*).

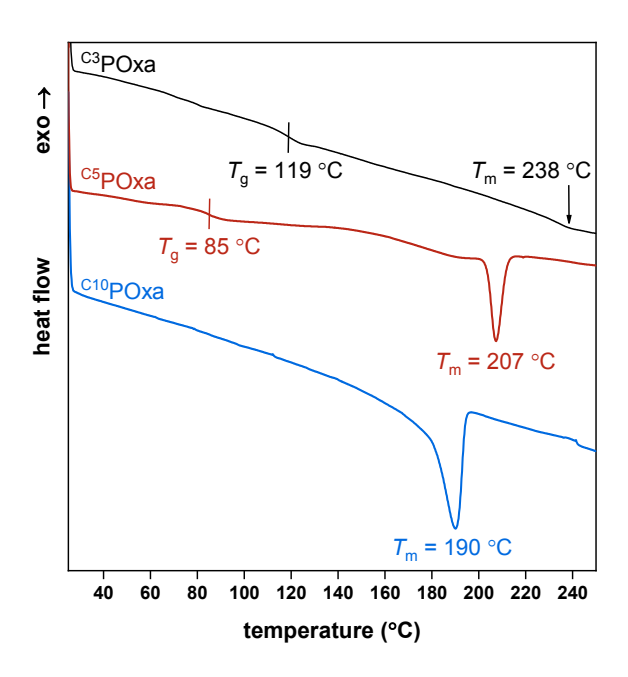


Figure 3. DSC thermograms of POxa showing the effect of SGs on $T_{\rm g}$ and $T_{\rm m}$.

The POxa were all semicrystalline, likely due to the stereoregular backbone, which was exciting because crystallinity is uncommon for POxa¹³ and for non-isocyanate PUs in general.^{57–62} Therefore, these polymers could access different properties, such as greater modulus and strength compared to fully amorphous polymers.⁶³ Longer SGs decreased $T_{\rm m}$ from 238 °C (C3) to 190 °C (C10) and resulted in qualitatively more crystalline materials (Figure 3). The observed $T_{\rm g}$ and $T_{\rm m}$ trends demonstrate that SGs provide a handle for tuning POxa thermal properties, in line with other types of polymers with alkyl side chains.^{64–68}

Conclusions. The addition of alkyl and alkoxy SGs successfully solubilized PHO and POxa containing a rigid spirocyclic linker in common organic solvents. This strategy enabled fully homogeneous polymerizations, molar mass determination by SEC, and structural characterization by solution-state 1D and 2D NMR spectroscopy. PHO and POxa exhibited surprising divergent solubility: PHO required strong hydrogen bond disruptors (i.e., DMF, DMSO, and HFIP) whereas POxa relied on SG hydrophobicity to facilitate solubility in less polar solvents (i.e., DCM and

CHCl₃). Additional trends were observed on the basis of SG structure within each polymer scaffold. The most dramatic differences occurred after cleaving the side chain of the most soluble PHO (i.e., SG = EHE) to form insoluble CH2PHO.

PHO displayed lower thermal stability than the corresponding POxa. TGA–MS analysis supported multiple PHO degradation pathways, including dehydration and reversion to less stable acyclic urethane linkages. SG length provided a handle for tuning POxa $T_{\rm g}$ while maintaining relatively high values (85–119 °C), as expected for this class of polymers. Unlike most POxa, these stereoregular polymers were semicrystalline with high $T_{\rm m}$'s (190–238 °C) that were influenced by SG length. This work provides a general strategy for achieving soluble POxa and improves fundamental understanding of structure–property relationships to inform the design of next generation high temperature thermoplastics.

ASSOCIATED CONTENT

Supporting Information.

The Supporting Information is available free of charge at

https://pubs.acs.org/doi/10.1021/acs.macromol.2c02104.

Additional polymer characterization, including SEC chromatograms, TGA and DSC

thermograms, TGA-MS data. Experimental details, including instrumentation, methods, reagent

sources, synthetic procedures, characterization of all new compounds. (PDF)

CIF file for ^{C5}bisαCC (CIF)

AUTHOR INFORMATION

Corresponding Author

Jessica R. Lamb – Department of Chemistry, University of

Minnesota—Twin Cities, Minneapolis, Minnesota 55455,

United States; orcid.org/0000-0001-9391-9515;

Email: jrlamb@umn.edu

Authors

Allison R. Wong – Department of Chemistry, University of

Minnesota—Twin Cities, Minneapolis, Minnesota 55455,

United States; orcid.org/0000-0002-2511-2098

Melissa Barrera – Department of Chemistry, University of

Minnesota—Twin Cities, Minneapolis, Minnesota 55455,

United States; orcid.org/0000-0001-7215-8366

Arpan Pal – Department of Chemistry, University of

Minnesota—Twin Cities, Minneapolis, Minnesota 55455,

United States; orcid.org/0000-0002-7985-0598

Complete contact information is available at:

https://pubs.acs.org/10.1021/acs.macromol.2c02104

Notes

The authors declare no competing financial interest.

A preprint of this article appeared on ChemRxiv at DOI: 10.26434/chemrxiv-2022-1crdw.

ACKNOWLEDGMENTS

This work was supported by National Science Foundation (NSF) Center for Sustainable Polymers, which is an NSF-supported Center for Chemical Innovation (CHE-1901635) and the University of Minnesota (UMN). We thank Prof. Julia Kalow and Ian Pierce for assistance with TGA-MS data

collection and Le Dung Pham for assistance with X-ray diffraction data collection. X-ray diffraction analysis was performed using a crystal diffractometer acquired through an NSF-MRI award (CHE-1229400) in the X-ray laboratory at UMN supervised by Dr. Victor G. Young, Jr. NMR analysis was supported by the Office of the Vice President of Research (OVPR), College of Science and Engineering (CSE), the Department of Chemistry at UMN, and the Office of the Director, National Institutes of Health (NIH, S100D011952). Mass spectrometry analysis was performed at the UMN Department of Chemistry Mass Spectrometry Laboratory (MSL), supported by OVRP, CSE, and the Department of Chemistry at UMN, as well as the NSF (CHE-1336940). TGA–MS experiments made use of the IMSERC Physical Characterization facility at Northwestern University, which has received support from the Soft and Hybrid Nanotechnology Experimental (SHyNE) Resource (NSF ECCS-2025633), and Northwestern University. The content of this paper is the sole responsibility of the authors and does not represent the official views of or endorsement by the NIH, MSL, or NSF.

REFERENCES

- (1) Akindoyo, J. O.; Beg, M. D. H.; Ghazali, S.; Islam, M. R.; Jeyaratnam, N.; Yuvaraj, A. R. Polyurethane Types, Synthesis and Applications A Review. *RSC Adv.* **2016**, *6*, 114453–114482. https://doi.org/10.1039/c6ra14525f.
- (2) Engels, H. W.; Pirkl, H. G.; Albers, R.; Albach, R. W.; Krause, J.; Hoffmann, A.; Casselmann, H.; Dormish, J. Polyurethanes: Versatile Materials and Sustainable Problem Solvers for Today's Challenges. *Angew. Chem., Int. Ed.* **2013**, *52*, 9422–9441. https://doi.org/10.1002/anie.201302766.
 - (3) Gama, N. V.; Ferreira, A.; Barros-Timmons, A. Polyurethane Foams: Past, Present, and

Future. Materials 2018, 11, 1841. https://doi.org/10.3390/ma11101841.

- (4) Chattopadhyay, D. K.; Raju, K. V. S. N. Structural Engineering of Polyurethane Coatings for High Performance Applications. *Prog. Polym. Sci.* **2007**, *32*, 352–418. https://doi.org/10.1016/j.progpolymsci.2006.05.003.
- (5) Golling, F. E.; Pires, R.; Hecking, A.; Weikard, J.; Richter, F.; Danielmeier, K.; Dijkstra, D. Polyurethanes for Coatings and Adhesives Chemistry and Applications. *Polym. Int.* **2019**, *68*, 848–855. https://doi.org/10.1002/pi.5665.
- (6) Prisacariu, C. Polyurethane Elastomers: From Morphology to Mechanical Aspects; Springer: New York, 2011.
- (7) Kordomenos, P. I.; Kresta, J. E.; Frisch, K. C. Thermal Stability of Isocyanate-Based Polymers. 2. Kinetics of the Thermal Dissociation of Model Urethane, Oxazolidone, and Isocyanurate Block Copolymers. *Macromolecules* **1987**, *20*, 2077–2083. https://doi.org/10.1021/ma00175a006.
- (8) Sendijarevic, V.; Sendijarevic, A.; Lekovic, H.; Lekovic, H.; Frisch, K. C. Polyoxazolidones for High Temperature Applications. *J. Elastomers Plast.* **1996**, *28*, 63–83. https://doi.org/10.1177/009524439602800104.
- (9) Prokofyeva, A.; Laurenzen, H.; Dijkstra, D. J.; Frick, E.; Schmidt, A. M.; Guertler, C.; Koopmans, C.; Wolf, A. Poly-2-Oxazolidones with Tailored Physical Properties Synthesized by Catalyzed Polyaddition of 2,4-Toluene Diisocyanate and Different Bisphenol-Based Diepoxides. *Polym. Int.* **2017**, *66*, 399–404. https://doi.org/10.1002/pi.5279.
 - (10) Kim, N. K.; Sogawa, H.; Yamamoto, K.; Hayashi, Y.; Kawauchi, S.; Takata, T. DBU-

- Mediated Highly Efficient CO₂-Fixation to Propargylamines and Polypropargylamine. *Chem. Lett.* **2018**, *47*, 1063–1066. https://doi.org/10.1246/cl.180477.
- (11) Habets, T.; Siragusa, F.; Grignard, B.; Detrembleur, C. Advancing the Synthesis of Isocyanate-Free Poly(Oxazolidones)s: Scope and Limitations. *Macromolecules* **2020**, *53*, 6396–6408. https://doi.org/10.1021/acs.macromol.0c01231.
- (12) Altmann, H. J.; Clauss, M.; König, S.; Frick-Delaittre, E.; Koopmans, C.; Wolf, A.; Guertler, C.; Naumann, S.; Buchmeiser, M. R. Synthesis of Linear Poly(Oxazolidin-2-One)s by Cooperative Catalysis Based on *N*-Heterocyclic Carbenes and Simple Lewis Acids. *Macromolecules* **2019**, *52*, 487–494. https://doi.org/10.1021/acs.macromol.8b02403.
- (13) Herweh, J. E.; Whitmore, W. Y. Poly-2-Oxazolidones: Preparation and Characterization. *J. Polym. Sci., Part A: Polym. Chem.* **1970**, 8, 2759–2773. https://doi.org/10.1002/pol.1970.150081004.
- (14) Harris, F. W.; Gupta, R. K. Synthesis and Intramolecular Cyclization of Ethynyl-Substituted Polyurethanes. *Polym. Prepr. (Am. Chem. Soc., Div. Polym. Chem.)* **1981**, *22*, 25–26.
- (15) Pankratov, V. A.; Frenkel, T. M.; Fainleib, A. M. 2-Oxazolidinones. *Russ. Chem. Rev.* **1983**, *52*, 576–593.
- (16) Iwakura, Y.; Nabeya, A.; Hayano, F. Polyoxazolidones. *J. Polym. Sci., Part A: Polym. Chem.* **1967**, *5*, 1865–1880. https://doi.org/10.1002/pol.1967.150050805.
- (17) Pelzer, T.; Eling, B.; Thomas, H. J.; Luinstra, G. A. Toward Polymers with Oxazolidin-2-One Building Blocks through Tetra-*n*-Butyl-Ammonium Halides (Cl, Br, I) Catalyzed Coupling of Epoxides with Isocyanates. *Eur. Polym. J.* **2018**, *107*, 1–8.

https://doi.org/10.1016/j.eurpolymj.2018.07.039.

- (18) Parthipan, B.; Mahadevan, A. Effects of Methylisocyanate on Soil Microflora and the Biochemical Activity of Soils. *Environ. Pollut.* **1995**, *87*, 283–287. https://doi.org/10.1016/0269-7491(94)P4159-L.
- (19) Baur, X.; Marek, W.; Ammon, J.; Czuppon, A. B.; Marczynski, B.; Raulf-Heimsoth, M.; Roemmelt, H.; Fruhmann, G. Respiratory and Other Hazards of Isocyanates. *Int. Arch. Occup. Environ. Health* **1994**, *66*, 141–152. https://doi.org/10.1007/BF00380772.
 - (20) Merenyi, S. Reach Regulation No 1907/2006 (May 2018); GRIN Verlag: Munich, 2018.
- (21) Iwakura, Y.; Izawa, S.-I.; Hayano, F. Polyoxazolidones Prepared from Bisurethans and Bisepoxides. *J. Polym. Sci., Part A: Polym. Chem.* **1966**, *4*, 751–760. https://doi.org/10.1002/pol.1966.150040402.
- (22) Wu, Q.; Chen, J.; Guo, X.; Xu, Y. Copper(I)-Catalyzed Four-Component Coupling Using Renewable Building Blocks of CO₂ and Biomass-Based Aldehydes. *Eur. J. Org. Chem.* **2018**, 2018, 3105–3113. https://doi.org/10.1002/ejoc.201800461.
- (23) Kim, N. K.; Sogawa, H.; Felicia, M. D.; Takata, T. DBU-Catalyzed CO₂ Fixation in Polypropargylamines under Solvent-Free Conditions. *Polym. J.* **2019**, *51*, 351–357. https://doi.org/10.1038/s41428-018-0125-8.
- (24) Teffahi, D.; Hocine, S.; Li, C.-J. Synthesis of Oxazolidinones, Dioxazolidinone and Polyoxazolidinone (a New Polyurethane) via a Multi Component-Coupling of Aldehyde, Diamine Dihydrochloride, Terminal Alkyne and CO₂. *Lett. Org. Chem.* **2012**, *9*, 585–593. https://doi.org/10.1002/chin.201308127.

- (25) Ngassam Tounzoua, C.; Grignard, B.; Detrembleur, C. Exovinylene Cyclic Carbonates: Multifaceted CO2-Based Building Blocks for Modern Chemistry and Polymer Science. *Angew. Chem., Int. Ed.* **2022**, *61*, e202116066. https://doi.org/10.1002/anie.202116066.
- (26) Gennen, S.; Grignard, B.; Tassaing, T.; Jérôme, C.; Detrembleur, C. CO₂-Sourced α-Alkylidene Cyclic Carbonates: A Step Forward in the Quest for Functional Regioregular Poly(Urethane)s and Poly(Carbonate)s. *Angew. Chem., Int. Ed.* **2017**, *56*, 10394–10398. https://doi.org/10.1002/anie.201704467.
- (27) Artz, J.; Müller, T. E.; Thenert, K.; Kleinekorte, J.; Meys, R.; Sternberg, A.; Bardow, A.; Leitner, W. Sustainable Conversion of Carbon Dioxide: An Integrated Review of Catalysis and Life Cycle Assessment. *Chem. Rev.* **2018**, *118*, 434–504. https://doi.org/10.1021/acs.chemrev.7b00435.
- (28) Grignard, B.; Gennen, S.; Jérôme, C.; Kleij, A. W.; Detrembleur, C. Advances in the Use of CO₂ as a Renewable Feedstock for the Synthesis of Polymers. *Chem. Soc. Rev.* **2019**, *48*, 4466–4514. https://doi.org/10.1039/c9cs00047j.
- (29) Mei, J.; Bao, Z. Side Chain Engineering in Solution-Processable Conjugated Polymers. *Chem. Mater.* **2014**, *26*, 604–615. https://doi.org/10.1021/cm4020805.
- (30) Bhattacharya, A.; De, A. Conducting Polymers in Solution Progress toward Processibility. *J. Macromol. Sci. Rev. Macromol. Chem. Phys.* **1999**, *39*, 17–56. https://doi.org/10.1081/mc-100101416.
- (31) Li, M.; Leenaers, P. J.; Wienk, M. M.; Janssen, R. A. J. The Effect of Alkyl Side Chain Length on the Formation of Two Semi-Crystalline Phases in Low Band Gap Conjugated Polymers.

- *J. Mater. Chem. C* **2020**, *8*, 5856–5867. https://doi.org/10.1039/d0tc00172d.
- (32) Chen, M. S.; Lee, O. P.; Niskala, J. R.; Yiu, A. T.; Tassone, C. J.; Schmidt, K.; Beaujuge, P. M.; Onishi, S. S.; Toney, M. F.; Zettl, A.; Fréchet, J. M. J. Enhanced Solid-State Order and Field-Effect Hole Mobility through Control of Nanoscale Polymer Aggregation. *J. Am. Chem. Soc.* **2013**, *135*, 19229–19236. https://doi.org/10.1021/ja4088665.
- (33) Egbe, D. A. M.; Türk, S.; Rathgeber, S.; Kühnlenz, F.; Jadhav, R.; Wild, A.; Birckner, E.; Adam, G.; Pivrikas, A.; Cimrova, V.; Knör, G.; Sariciftci, N. S.; Hoppe, H. Anthracene Based Conjugated Polymers: Correlation between π–π-Stacking Ability, Photophysical Properties, Charge Carrier Mobility, and Photovoltaic Performance. *Macromolecules* **2010**, *43*, 1261–1269. https://doi.org/10.1021/ma902273s.
- (34) Chen, Z.; Yan, L.; Rech, J. J.; Hu, J.; Zhang, Q.; You, W. Green-Solvent-Processed Conjugated Polymers for Organic Solar Cells: The Impact of Oligoethylene Glycol Side Chains. *ACS Appl. Polym. Mater.* **2019**, *I*, 804–814. https://doi.org/10.1021/acsapm.9b00044.
- (35) Pelckmans, M.; Renders, T.; Van De Vyver, S.; Sels, B. F. Bio-Based Amines through Sustainable Heterogeneous Catalysis. *Green Chem.* **2017**, *19*, 5303–5331. https://doi.org/10.1039/c7gc02299a.
- (36) Gupta, N. K.; Reif, P.; Palenicek, P.; Rose, M. Toward Renewable Amines: Recent Advances in the Catalytic Amination of Biomass-Derived Oxygenates. *ACS Catal.* **2022**, *12*, 10400–10440. https://doi.org/10.1021/acscatal.2c01717.
- (37) Nielsen, A. T.; Carpenter, W. R. 1,4-Cyclohexanedione. *Org. Synth.* **1965**, *45*, 25. https://doi.org/10.15227/orgsyn.045.0025.

- (38) Verma, M.; Mandyal, P.; Singh, D.; Gupta, N. Recent Developments in Heterogeneous Catalytic Routes for the Sustainable Production of Succinic Acid from Biomass Resources. *ChemSusChem* **2020**, *13*, 4026–4034. https://doi.org/10.1002/cssc.202000690.
- (39) Reid, D. R.; Jackson, N. E.; Bourque, A. J.; Snyder, C. R.; Jones, R. L.; De Pablo, J. J. Aggregation and Solubility of a Model Conjugated Donor-Acceptor Polymer. *J. Phys. Chem. Lett.* **2018**, *9*, 4802–4807. https://doi.org/10.1021/acs.jpclett.8b01738.
- (40) Yoshida, M.; Hayashi, M.; Shishido, K. Palladium-Catalyzed Diastereoselective Coupling of Propargylic Oxiranes with Terminal Alkynes. *Org. Lett.* **2007**, *9*, 1643–1646. https://doi.org/10.1021/ol070224n.
- (41) Komatsuki, K.; Kozuma, A.; Saito, K.; Yamada, T. Decarboxylative Nazarov Cyclization-Based Chirality Transfer for Asymmetric Synthesis of 2-Cyclopentenones. *Org. Lett.* **2019**, *21*, 6628–6632. https://doi.org/10.1021/acs.orglett.9b02107.
- (42) Reif, B.; Ashbrook, S. E.; Emsley, L.; Hong, M. Solid-State NMR Spectroscopy. *Nat. Rev. Methods Primers* **2021**, *1*, 2. https://doi.org/10.1038/s43586-020-00002-1.
- (43) Nishi, K.; Hiroi, T.; Hashimoto, K.; Fujii, K.; Han, Y. S.; Kim, T. H.; Katsumoto, Y.; Shibayama, M. SANS and DLS Study of Tacticity Effects on Hydrophobicity and Phase Separation of Poly(*N*-Isopropylacrylamide). *Macromolecules* **2013**, *46*, 6225–6232. https://doi.org/10.1021/ma401349v.
- (44) Mrkvičková, L.; Stêjskal, J.; Spěváček, J.; Horská, J.; Quadrat, O. Aggregation Behavior of Stereoregular Poly(Methyl Methacrylates) in Dilute Solution: Light Scattering and Proton N.M.R. Study. *Polymer* **1983**, *24*, 700–706. https://doi.org/10.1016/0032-3861(83)90006-X.

- (45) Lucas, J. M.; Labastide, J. A.; Wei, L.; Tinkham, J. S.; Barnes, M. D.; Lahti, P. M. Carpenter's Rule Folding in Rigid-Flexible Block Copolymers with Conjugation-Interrupting, Flexible Tethers between Oligophenylenevinylenes. *J. Phys. Chem. A* **2015**, *119*, 8010–8020. https://doi.org/10.1021/acs.jpca.5b02295.
- (46) Habets, T.; Siragusa, F.; Grossman, Q.; Grignard, B.; Detrembleur, C. Facile Construction of Functional Poly(Monothiocarbonate) Copolymers under Mild Operating Conditions. *Polym. Chem.* **2022**, *13*, 3076–3090. https://doi.org/10.1039/d2py00307d.
- (47) Hoffmann, R. W. Allylic 1,3-Strain as a Controlling Factor in Stereoselective Transformations. *Chem. Rev.* **1989**, *89*, 1841–1860. https://doi.org/10.1021/cr00098a009.
- (48) *Handbook of Chemistry and Physics*, 100th ed.; Rumble, J. R., Lide, D. R., Bruno, T. J., Eds.; CRC Press, Taylor and Francis Group: Boca Raton, FL, 2019.
- (49) Berkessel, A.; Adrio, J. A.; Hüttenhain, D.; Neudörfl, J. M. Unveiling the "Booster Effect" of Fluorinated Alcohol Solvents: Aggregation-Induced Conformational Changes and Cooperatively Enhanced H-Bonding. *J. Am. Chem. Soc.* **2006**, *128*, 8421–8426. https://doi.org/10.1021/ja0545463.
- (50) Kamlet, M. J.; Abboud, J. L. M.; Abraham, M. H.; Taft, R. W. Linear Solvation Energy Relationships. 23. A Comprehensive Collection of the Solvatochromic Parameters, π^* , α , and β , and Some Methods for Simplifying the Generalized Solvatochromic Equation. *J. Org. Chem.* **1983**, 48, 2877–2887. https://doi.org/10.1021/jo00165a018.
- (51) Topuz, F.; Uyar, T. Influence of Hydrogen-Bonding Additives on Electrospinning of Cyclodextrin Nanofibers. *ACS Omega* **2018**, *3*, 18311–18322.

https://doi.org/10.1021/acsomega.8b02662.

- (52) Du, M. X.; Yuan, Y. F.; Zhang, J. M.; Liu, C. Y. Hydrogen-Bonding Interactions in Polymer-Organic Solvent Mixtures. *Macromolecules* **2022**, *55*, 4578–4588. https://doi.org/10.1021/acs.macromol.2c00799.
- (53) He, Y.; Eloi, J. C.; Harniman, R. L.; Richardson, R. M.; Whittell, G. R.; Mathers, R. T.; Dove, A. P.; O'Reilly, R. K.; Manners, I. Uniform Biodegradable Fiber-Like Micelles and Block Comicelles via "Living" Crystallization-Driven Self-Assembly of Poly(L-Lactide) Block Copolymers: The Importance of Reducing Unimer Self-Nucleation via Hydrogen Bond Disruption. *J. Am. Chem. Soc.* **2019**, *141*, 19088–19098. https://doi.org/10.1021/jacs.9b09885.
- (54) Duan, C.; Willems, R. E. M.; Van Francker, J. J.; Bruijnaers, B. J.; Wienk, M. M.; Janssen, R. A. J. Effect of Side Chain Length on the Charge Transport, Morphology, and Photovoltaic Performance of Conjugated Polymers in Bulk Heterojunction Solar Cells. *J. Mater. Chem. A* **2016**, *4*, 1855–1866. https://doi.org/10.1039/c5ta09483f.
- (55) Yiu, A. T.; Beaujuge, P. M.; Lee, O. P.; Woo, C. H.; Toney, M. F.; Fréchet, J. M. J. Side-Chain Tunability of Furan-Containing Low-Band-Gap Polymers Provides Control of Structural Order in Efficient Solar Cells. *J. Am. Chem. Soc.* **2012**, *134*, 2180–2185. https://doi.org/10.1021/ja2089662.
- (56) Kordomenos, P. I.; Kresta, J. E. Thermal Stability of Isocyanate-Based Polymers. 1. Kinetics of the Thermal Dissociation of Urethane, Oxazolidinone, and Isocyanurate Groups. *Macromolecules* **1981**, *14*, 1434–1437. https://doi.org/10.1021/ma50006a056.
 - (57) Li, S.; Sang, Z.; Zhao, J.; Zhang, Z.; Cheng, J.; Zhang, J. Synthesis and Properties of Non-

Isocyanate Aliphatic Crystallizable Thermoplastic Poly(Ether Urethane) Elastomers. *Eur. Polym. J.* **2016**, *84*, 784–798. https://doi.org/10.1016/j.eurpolymj.2016.08.007.

- (58) Bähr, M.; Bitto, A.; Mülhaupt, R. Cyclic Limonene Dicarbonate as a New Monomer for Non-Isocyanate Oligo- and Polyurethanes (NIPU) Based upon Terpenes. *Green Chem.* **2012**, *14*, 1447–1454. https://doi.org/10.1039/c2gc35099h.
- (59) Schimpf, V.; Max, J. B.; Stolz, B.; Heck, B.; Mülhaupt, R. Semicrystalline Non-Isocyanate Polyhydroxyurethanes as Thermoplastics and Thermoplastic Elastomers and Their Use in 3D Printing by Fused Filament Fabrication. *Macromolecules* **2019**, *52*, 320–331. https://doi.org/10.1021/acs.macromol.8b01908.
- (60) Duval, C.; Kébir, N.; Jauseau, R.; Burel, F. Organocatalytic Synthesis of Novel Renewable Non-Isocyanate Polyhydroxyurethanes. *J. Polym. Sci., Part A: Polym. Chem.* **2016**, *54*, 758–764. https://doi.org/10.1002/pola.27908.
- (61) Deng, Y.; Li, S.; Zhao, J.; Zhang, Z.; Zhang, J.; Yang, W. Crystallizable and Tough Aliphatic Thermoplastic Poly(Ether Urethane)s Synthesized through a Non-Isocyanate Route. *RSC Adv.* **2014**, *4*, 43406–43414. https://doi.org/10.1039/c4ra05880a.
- (62) Li, S.; Zhao, J.; Zhang, Z.; Zhang, J.; Yang, W. Synthesis and Characterization of Aliphatic Thermoplastic Poly(Ether Urethane) Elastomers through a Non-Isocyanate Route. *Polymer* **2015**, 57, 164–172. https://doi.org/10.1016/j.polymer.2014.12.009.
- (63) Bigg, D. M. Mechanical Property Enhancement of Semicrystalline Polymers—A Review. *Polym. Eng. Sci.* **1988**, *28*, 830–841. https://doi.org/10.1002/pen.760281303.
 - (64) Guo, Y. T.; Shi, C.; Du, T. Y.; Cheng, X. Y.; Du, F. S.; Li, Z. C. Closed-Loop Recyclable

Aliphatic Poly(Ester-Amide)s with Tunable Mechanical Properties. *Macromolecules* **2022**, *55*, 4000–4010. https://doi.org/10.1021/acs.macromol.2c00221.

- (65) Baker, G. L.; Vogel, E. B.; Smith, M. R. Glass Transitions in Polylactides. *Polym. Rev.*2008, 48, 64–84. https://doi.org/10.1080/15583720701834208.
- (66) Rogers, S.; Mandelkern, L. Glass Transitions of the Poly-(*n*-Alkyl Methacrylates). *J. Phys. Chem.* **1957**, *61*, 985–991. https://doi.org/10.1021/j150553a033.
- (67) Song, Y.; Ji, X.; Dong, M.; Li, R.; Lin, Y. N.; Wang, H.; Wooley, K. L. Advancing the Development of Highly-Functionalizable Glucose-Based Polycarbonates by Tuning of the Glass Transition Temperature. *J. Am. Chem. Soc.* **2018**, *140*, 16053–16057. https://doi.org/10.1021/jacs.8b10675.
- (68) Wang, X.; Jeong, Y. L.; Love, C.; Stretz, H. A.; Stein, G. E.; Long, B. K. Design, Synthesis, and Characterization of Vinyl-Addition Polynorbornenes with Tunable Thermal Properties. *Polym. Chem.* **2021**, *12*, 5831–5841. https://doi.org/10.1039/d1py01050f.